The Plant Journal (2007) **52**, 485–498 doi: 10.1111/j.1365-313X.2007.03252.x

Characterization of Arabidopsis ABCG11/WBC11, an ATP binding cassette (ABC) transporter that is required for cuticular lipid secretion†

David Bird[1], Fred Beisson[2], Alexandra Brigham[1], John Shin[1], Stephen Greer[1], Reinhard Jetter[1,4], Ljerka Kunst[1], Xuemin Wu[1], Alexander Yephremov[3] and Lacey Samuels[1,*]

[1]*Department of Botany, University of British Columbia, Vancouver, BC, Canada V6T 1Z4,*
[2]*Department of Plant Biology, Michigan State University, East Lansing, MI 48824, USA,*
[3]*Max-Planck-Institut für Züchtungsforschung, 50829 Köln, Germany, and*
[4]*Department of Chemistry, University of British Columbia, Vancouver, BC, Canada V6T 1Z3*

Received 21 March 2007; revised 13 June 2007; accepted 28 June 2007.
*For correspondence (fax 604 822-6089; e-mail lsamuels@interchange.ubc.ca).
†This paper is dedicated to the memory of Vincent R. Franceschi (1953–2005).

Summary

ABCG11/WBC11, an ATP binding cassette (ABC) transporter from *Arabidopsis thaliana*, is a key component of the export pathway for cuticular lipids. Arabidopsis *wbc11* T-DNA insertional knock-out mutants exhibited lipidic inclusions inside epidermal cells similar to the previously characterized wax transporter mutant *cer5*, with a similar strong reduction in the alkanes of surface waxes. Moreover, the *wbc11* knock-out mutants also showed defects not present in *cer5*, including post-genital organ fusions, stunted growth and a reduction in cutin load on the plant surface. A mutant line previously isolated in a forward genetics screen, called *permeable leaves 1* (*pel1*), was identified as an allele of *ABCG11/WBC11*. The double knock-out *wbc11 cer5* exhibited the same morphological and biochemical phenotypes as the *wbc11* knock-out. A YFP-WBC11 fusion protein rescued a T-DNA knock-out mutant and was localized to the plasma membrane. These results show that WBC11 functions in secretion of surface waxes, possibly by interacting with CER5. However, unlike *ABCG12/CER5*, *ABCG11/WBC11* is important to the normal process of cutin formation.

Keywords: cuticle, wax, cutin, ABC transporter, cell wall, *Arabidopsis thaliana*.

Introduction

Aerial surfaces of the primary plant body are coated by a waxy cuticle that serves physiological, ecological and developmental roles. Its primary function is to act as a hydrophobic barrier limiting non-stomatal water loss, but it also provides an interface between the plant and the environment. For example, the cuticle surface can, to various degrees, repel water, and has therefore been implied in defense against pathogenic spores that require high humidity for germination (Neinhuis and Barthlott, 1997). In addition, the cuticle plays an important role in preventing post-genital organ fusion: plant lines overexpressing a fungal cutinase or carrying mutations that result in an alteration in cutin organization often have a '*fiddlehead*' phenotype, where fusions amongst floral organs deform the growing inflorescence (Nawrath, 2006). Plant cuticles consist of cutin, a lipid polyester, as well as intracuticular wax, which is embedded within the cutin matrix, and epicuticular wax, which is deposited on the surface of the cuticle (Jetter *et al.*, 2000).

Cutin is a polymer of fatty acid derivatives that are ester-linked and, possibly through cross-linking with glycerol, form a complex three-dimensional matrix (Graça *et al.*, 2002; Nawrath, 2002; Stark and Tian, 2006). In Arabidopsis this polymer is primarily made up of dicarboxy-, hydroxy- and dihydroxy- C16 and C18 fatty acids (Bonaventure *et al.*, 2004; Franke *et al.*, 2005; Xiao *et al.*, 2004). Plant cuticular wax typically consists of homologous series of very long chain fatty acid derivatives, as well as diverse terpenoid and phenolic components, depending upon the species, organ and developmental state (Jetter *et al.*, 2006).

Cuticular lipid biosynthesis is believed to occur exclusively within epidermal cells using plastid-derived C16 and

C18 fatty acids (Browse and Somerville, 1991; Nawrath, 2002). It is likely that cutin monomer biosynthesis is, at least in part, localized to the endoplasmic reticulum (ER) as the C16 and C18 fatty acids subsequently undergo a number of microsomal hydroxylation steps (Kolattukudy, 1984), one of which is performed by the cytochrome P450 CYP86A8 (LACERATA), an ω-hydroxylase required for normal cuticle formation (Wellesen *et al.*, 2001). Similar to cutin biosynthesis, wax biosynthesis has been localized to the ER, as demonstrated by GFP fusions of enzymes required for cuticular wax production such as CER6 and CER10 (Kunst and Samuels, 2003; Zheng *et al.*, 2005). Similarly, the fatty acyl-CoA reductase required for wax primary alcohols and esters, CER4, is also localized to the ER when expressed in yeast (Rowland *et al.*, 2006).

How the cutin and wax components are exported from the epidermal cell and assembled into the complex, three-dimensional, hydrophobic structure on the plant surface is not well understood. Although nothing is known about cutin precursor export, a single ATP binding cassette (ABC) transporter, CER5, has been shown to be involved in wax transport in Arabidopsis (Pighin *et al.*, 2004). The stems of *cer5-1*, and stems of a knock-out mutant *cer5-2*, still had 41% of the wild-type wax load, suggesting that additional transporters are involved in wax secretion to the surface (Pighin *et al.*, 2004). No other elements of the wax export machinery have been identified to date.

CER5 is a member of the WBC subfamily of Arabidopsis ABC transporters (Sanchez-Fernandez *et al.*, 2001), named after the canonical *WHITE-BROWN* complex of *Drosophila melanogaster* (Ewart *et al.*, 1994). It is also designated as ABCG12 for its similarity to the human lipidic transporters of the ABCG subfamily. The human ABCG subfamily members are emerging as important lipid transporters, including the sterol-transporting heterodimer ABCG5/ABCG8 and ABCG2, which forms a homodimer that functions in xenobiotic export (Wang *et al.*, 2006; Xu *et al.*, 2004). ABCG/WBC-type proteins are believed to be 'half'-transporters, requiring a second ABCG/WBC polypeptide to create a fully functional ABC transporter with two ABC and two transmembrane domains (Dreesen *et al.*, 1988). This subfamily provides interesting candidates for the additional wax exporters that must exist to account for the presence of cuticular wax in the *cer5* loss-of-function mutant.

Many ABC transporter genes show a high level of expression in the stem epidermis (Suh *et al.*, 2005). To pinpoint ABC transporters involved in cuticular lipid export within the WBC subfamily, we evaluated candidates with high expression in the stem epidermis for similar patterns of gene expression with *CER5* by applying a Genevestigator (Zimmermann *et al.*, 2004) gene expression correlation approach. Using 673 microarray data sets from aerial organs, we identified an ABC transporter *WBC11* (At1g17840) that showed a high degree of correlation with *CER5* (R^2 = 0.83) as a prime candidate for further analysis.

The objective of this study was to assess the function of WBC11 in cuticular lipid export using a reverse genetics approach. Our results show that mutations in *WBC11* cause reduced wax load and accumulation of intracellular lipidic inclusions. Surprisingly, mutations in *WBC11* also result in dwarfism, sterility, post-genital organ fusions and reduced cutin load.

Results

Genetic characterization of mutant alleles of WBC11

Three T-DNA insertional mutants lines, *wbc11-1*, *-2* and *-3,* were obtained from the Salk Institute and characterized in this study (Alonso *et al.*, 2003; Figure 1a). The two alleles *wbc11-1* and *wbc11-2* had T-DNA insertions 404 and 346 base pairs upstream of the predicted translation start site, respectively, and both showed a reduction, but not elimination, of gene transcript. The *wbc11-3* allele is an insertion at the 141st base pair of the 6th exon, which resulted in no detectable *WBC11* transcript (Figure 1b).

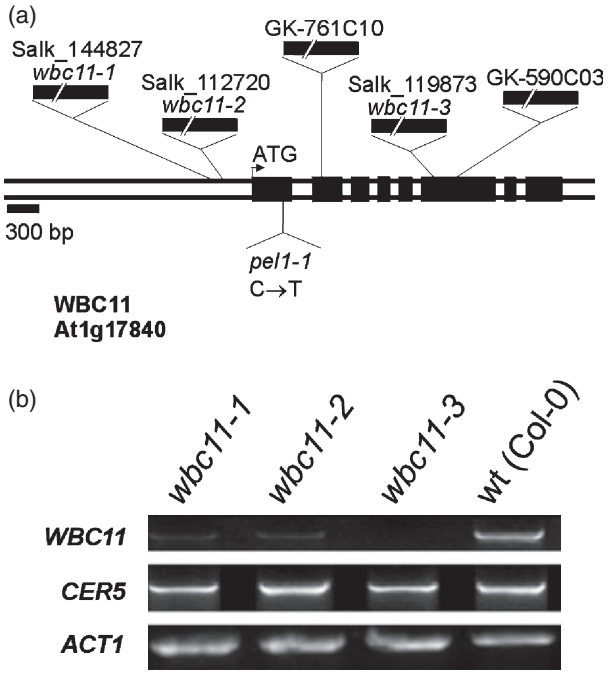

Figure 1. Mutant alleles of *WBC11*.
(a) The locations of T-DNA insertions and *pel1-1 WBC11* are mapped: *wbc11-1, -2* and *-3* are Salk T-DNA insertions in the 5′ untranslated region (UTR) (*wbc11-1* and *-2*) and 6th exon (*wbc11-3*). 761C10 and 590C03 are GABI-KAT T-DNA lines in the 2nd and 6th exons, respectively. The mutant *pel1-1* is a point mutant in the 1st intron that creates a premature stop codon at amino acid 97. Exons are shown as black boxes.
(b) Semiquantitative RT-PCR of steady-state *WBC11* and *CER5* mRNA in *wbc11* mutants compared with wild-type Columbia-0. Expression of *ACTIN1* was used as a loading control for the corresponding lanes above. RNA was isolated from stem tissue.

Using a toluidine blue test for detection of cuticular defects, Tanaka *et al.* (2004) identified seven *permeable leaves* (*pel*) mutants. The *pel1* genetic locus was mapped to the upper arm of chromosome 1 to a contig comprising 12 overlapping bacterial artificial chromosome (BAC) clones. In the positional candidate gene approach, we examined phenotypes of more than 20 loss-of-function T-DNA mutants from the corresponding region, and found that only two insertion mutants in At1g17840 (ecotype Columbia, Col-0, lines GK-590C03 and GK-761C10; Rosso *et al.*, 2003) showed organ fusion defects typical for some cuticular mutants, a reduced cuticular wax load and produced non-fertile flowers. For the allelism test, *pel1-1* heterozygotes (ecotype Ler) were pollinated by GK-590C03 plants heterozygous at the At1g17840 locus. Progeny resembling the *pel1-1* line segregated in a 46:15 (wild type : *pel1-1* mutant) ratio. This is consistent with the expected 3:1 ratio ($\chi^2 = 0.0055$, $P = 0.941$), indicating that *pel1-1* is another allele of the At1g17840 gene. Sequencing of genomic DNA confirmed that the *pel1* mutant allele has a C-to-T transition resulting in a premature UGA stop codon at amino acid position 97.

Mutations in WBC11 *cause reduced growth and post-genital organ fusions*

Plants homozygous for *wbc11-3* were dramatically smaller than wild-type plants, with rosette leaves rarely exceeding 0.5 cm in length. In addition to their reduced size, rosette leaves were misshapen and occasional leaf–leaf fusions were observed (Figure 2a, inset). At maturity, *wbc11-3* stems were very slender and highly branching, ending in terminal sterile flowers (Figure 2a). The two alleles with decreased, but not eliminated, transcript levels, *wbc11-1* and *wbc11-2*, were normal in size, leaf shape and fertility (Figure 2b). When embryos were isolated from heterozygous *wbc11-3*/*WBC11* siliques, two populations of embryos were observed: of 109 embryos, 20 were smaller and less pigmented, consistent with a 3:1 phenotypic segregation of a single recessive allele ($\chi^2 = 2.57$, $P = 0.109$; Figure 2c).

The knock-down mutants, *wbc11-1* and -2 had extensive organ fusions, many of which showed a *fiddlehead*-like phenotype resulting from stem–stem and stem–leaf fusions (Figure 2b). At such fusion sites, the outer periclinal wall of the epidermal cells adhered to the corresponding cells of adjacent organs. In some cases, the strength of the adhesion led to the epidermis being stretched between the adjacent stems (Figure 3a,b). Tears in the stretched epidermis could be observed using scanning electron microscopy (Figure 3c, arrow). In *wbc11-3*, leaf–leaf fusions were commonly observed (Figure 3d). In addition, aberrations in leaf trichome morphology could be also observed: trichomes were commonly two-pronged instead of the normal tripartite shape and were also often stunted, misshapen or even collapsed (Figure 3d,e).

Mutations in WBC11 *cause reduced cuticular wax and cutin loads*

To determine if disruptions in *WBC11* cause alterations in epicuticular wax, we examined wild-type (Col-0) and mutant

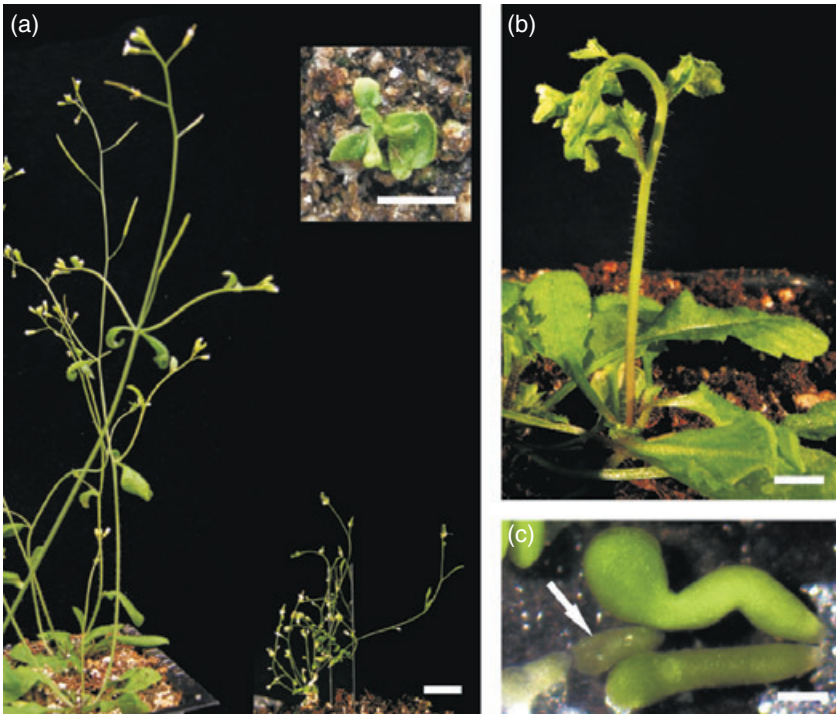

Figure 2. Phenotype of *wbc11* mutants of Arabidopsis showing reduced growth and post-genital organ fusions. Photographs (a and b) and photomicrograph (c).
(a) Seven-week-old *wbc11-3* plants (right) are smaller and often show deformed leaves and reduced apical dominance as compared with wild-type Columbia-0 plants (left).
(b) Six-week-old *wbc11-2* plants show stem–leaf fusions leading to a *fiddlehead*-like phenotype.
(c) Embryos segregated from heterozygous parents in a 3:1 ratio of embryos with wild-type phenotype and embryos with reduced size and pigmentation, presumably homozygous for the *wbc11-3* allele, respectively (arrows). Bars = 10 mm for (a) and (b), 200 μm for (c).

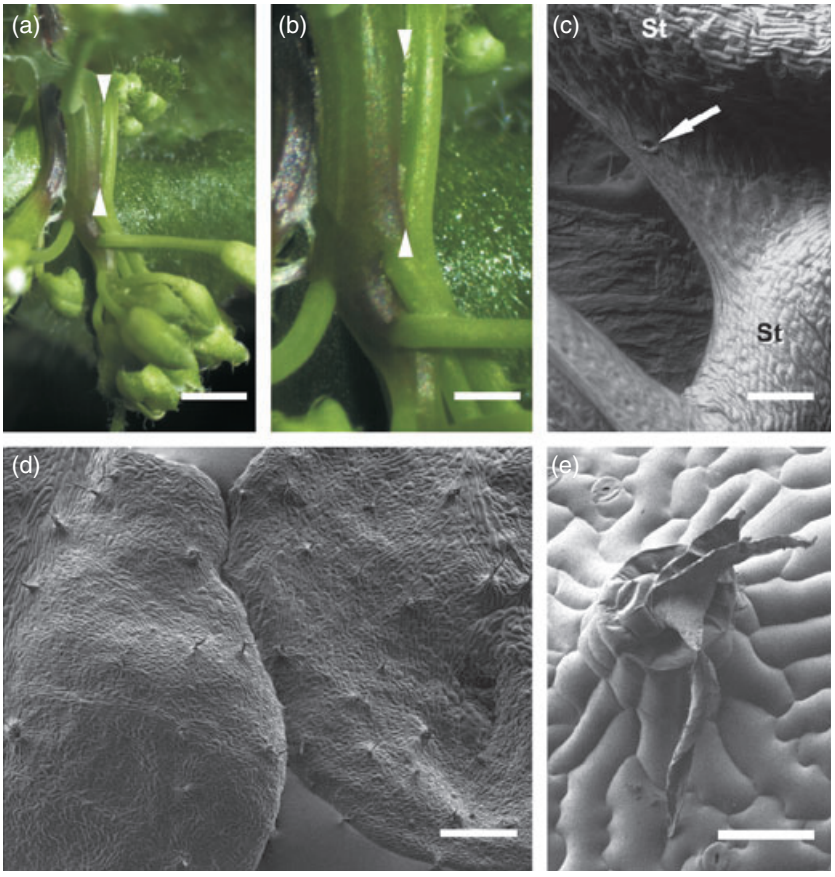

Figure 3. Phenotype of *wbc11* mutants showing post-genital organ fusions and leaf trichome defects. Photographs (a, b) and cryo-scanning electron micrographs (c–e) of fusions and deformed trichomes in *wbc11* mutants.
(a, b) Stem–stem post-genital organ fusions in *wbc11-2*. The fusion between two stems is shown between arrowheads. In some regions, the epidermis is being pulled apart.
(c) Stem–stem fusion in *wbc11-1* showing a tear in the stretched epidermis (arrow).
(d) Leaf–leaf fusion in *wbc11-3*. Trichomes in *wbc11-3* are stunted, collapsed or even absent.
(e) Collapsed trichome in *wbc11-3*. St = stem. Bars = 1 mm for (a), 0.5 mm for (b), 100 μm for (c), 500 μm for (d) and 25 μm for (e).

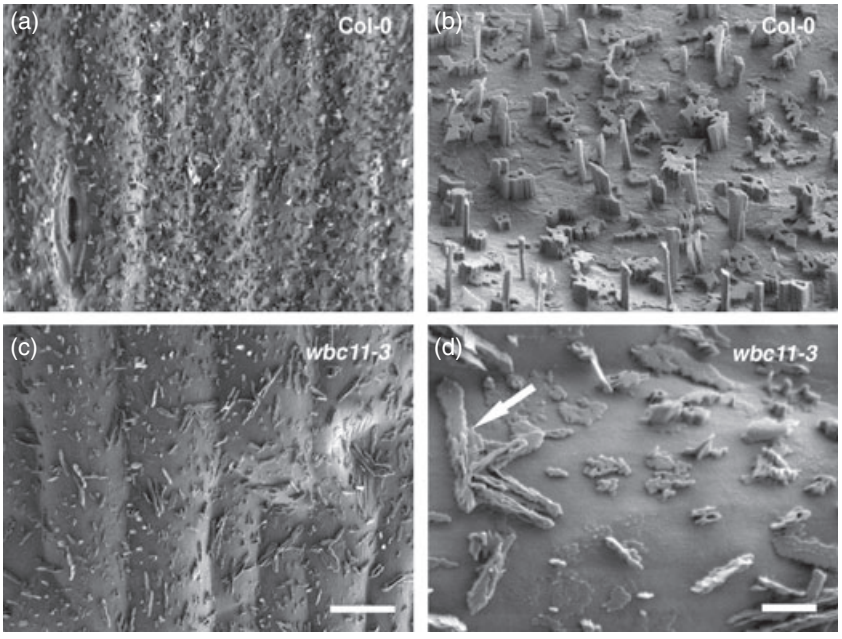

Figure 4. Epicuticular wax crystal density is lower on *wbc11-3* stems. Cryo-scanning electron micrographs showing epicuticular wax crystals in wild-type Columbia-0 (a, b) and *wbc11-3* (c, d) plants. The mutant *wbc11-3* has a lower density of crystals compared with wild type (c). Also, elongated, thickened plates are present on *wbc11-3* stems that were not found on wild-type stems. (d, arrow). Bars = 10 μm for (a, c) and 2 μm for (b, d).

stems by cryo-scanning electron microscopy (Figure 4). Consistent with the overall growth abnormalities, stem epidermal cells of *wbc11-3* were noticeably more irregular than those of wild type. Also, whereas plates, rods and columnar-shaped crystals were observed in both wild-type and mutant genotypes, only the *wbc-11-3* plants additionally

Table 1 Composition of cuticular waxes on inflorescence stems of Arabidopsis wild type (Col-0) and *wbc11* mutant lines. Mean values (μg cm^{-2}) of total wax loads and coverage of individual compound classes are given with SEs (n = 5)

	Total wax[a]	Fatty acids	Aldehydes	Alkanes[b]	Sec. alcohols	Ketone	Primary alcohols	Esters	Not identified
Col-0 (wild type)	19.5 ± 1.1	0.10 ± 0.04	0.48 ± 0.23	7.7 ± 0.4	2.1 ± 0.1	4.5 ± 0.2	1.7 ± 0.1	0.93 ± 0.13	1.4 ± 0.2
wbc11-1	7.9 ± 0.3	0.02 ± 0.01	0.10 ± 0.03	1.6 ± 0.2	1.2* ± 0.1	2.9* ± 0.1	1.0* ± 0.1	0.20* ± 0.03	0.6 ± 0.1
wbc11-2	9.1 ± 0.6	0.01 ± 0.007	0.16 ± 0.02	2.2 ± 0.4	1.5 ± 0.1	3.2* ± 0.2	1.0* ± 0.1	0.23* ± 0.02	0.7 ± 0.3
wbc11-3	9.3 ± 1.3	0.03 ± 0.007	0.10 ± 0.03	1.0 ± 0.2	2.5 ± 0.4	2.7 ± 0.7	0.4* ± 0.1	0.25 ± 0.13	2.2 ± 0.5
wbc11-3 cer5-2	9.9 ± 0.7	0.05 ± 0.01	0.20 ± 0.08	1.0 ± 0.1	2.3 ± 0.1	3.7 ± 0.1	0.6* ± 0.1	0.55 ± 0.05	1.4 ± 0.3

[a]Means are significantly different from each other (ANOVA, $F_{(4,20)}$ = 28.860, P < 0.001). Post hoc comparisons using Tukey's HSD test (P < 0.05) revealed that all mutants were significantly lower than wild type, but not different from each other.
[b]Means are significantly different from each other (ANOVA, $F_{(4,20)}$ = 101.324, P < 0.001). Post hoc comparisons using Tukey's HSD test (P < 0.05) revealed that all mutants were significantly lower than wild type; *wbc11-1* and *-2* were not significantly different from each other but were significantly larger than *wbc11-3* and *wbc11-3 cer5-2*.
*Values are significantly different from wild type (parametric means comparison using Games–Howell test, P < 0.05).

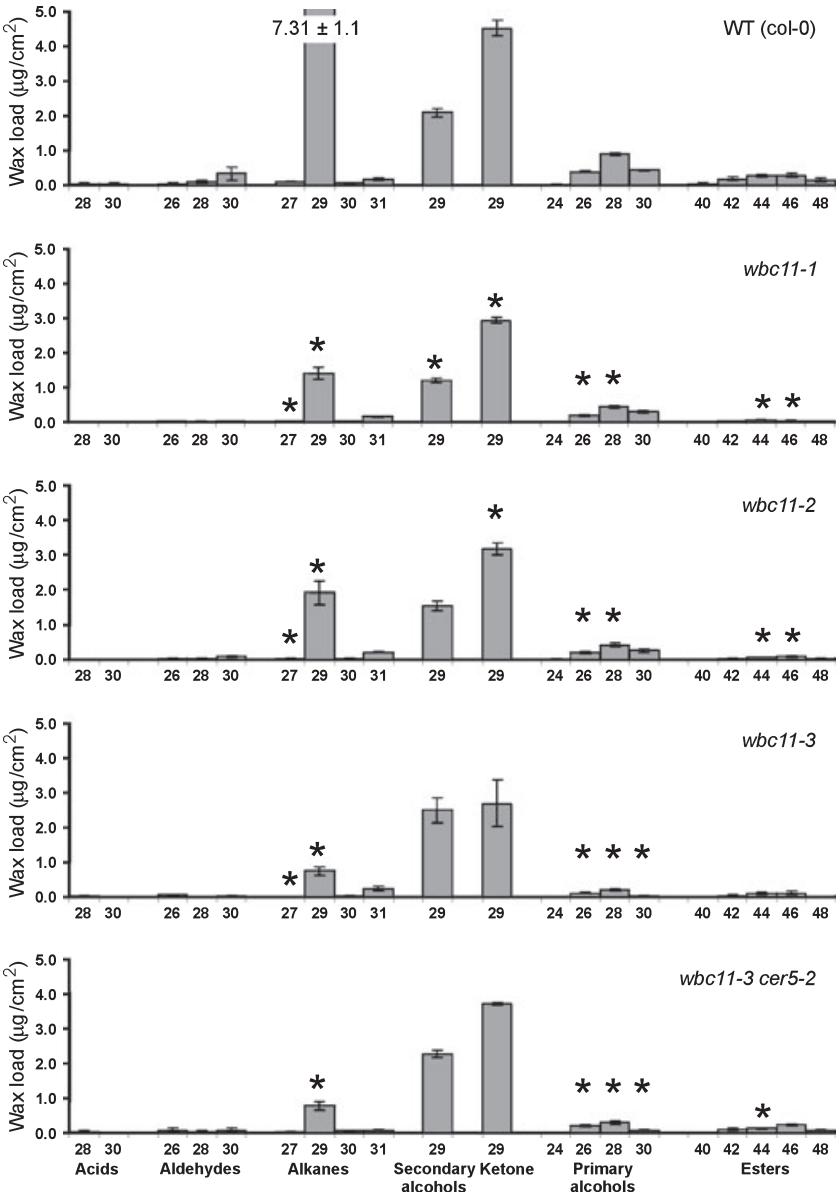

Figure 5. Epidermal wax load is reduced in *wbc11* stems. Sections of whole stems were chloroform extracted and analyzed for wax using GC-FID/MS. Wax loads are expressed in μg of wax per cm^2 of stem surface area. The genotype of each sample is shown in the upper right of the charts. Each wax constituent is designated by carbon chain length and is labeled by chemical class along the *x*-axis. Each value is the mean of five independent measurements of individual plants. *Means significantly different (P < 0.05) from wild type. Error bars = SE.

had thickened plates that appeared to be aggregated columnar-shaped crystals that were not observed in wild type (Figure 4d, arrow).

The reduced number of epicuticular wax crystals on the surface of *wbc11-3* suggested to us that *WBC11* may be involved in transport of wax components. To test this hypothesis, we examined the cuticular wax load and composition of stems from the *wbc11* alleles using gas chromatography with flame ionization detection (GC-FID). The total wax load (total chloroform-extractable lipids) in *wbc11-1*, *-2* and *3* was reduced by 41–56% compared with wild type (Col-0). Most of the change in wax load could be attributed to a 75–90% reduction of alkanes, the most abundant class of wax components on Arabidopsis stems (Table 1).

In all three mutant plant lines, the largest reduction was always observed in a single wax compound, nonacosane (C29 alkane; Figure 5). Furthermore, alkane levels in different *wbc11* alleles appeared to be correlated with the levels of detectable *WBC11* transcript in each line, that is, the knock-out allele *wbc11-3* had the strongest reduction in alkanes, which were significantly lower than those found in *wbc11-1* and *2* (Table 1). Significant reductions of C26 and C28 primary alcohols were also observed in all mutant lines. Also, significant reductions were observed in the C44 and C46 esters in the *wbc11-1* and *-2* knock-down alleles (Figure 5). In contrast, total loss of *WBC11* transcript in *wbc11-3* resulted in no significant change in the levels of C29 secondary alcohols and C29 ketone. In the *wbc11-1* line, these compounds were reduced, but relatively less so compared with the reduction of nonacosane (Figure 5).

Because *CER5* had also been implicated in wax secretion, and the knock-out *cer5-2* mutant had a similar reduction in wax load, predominantly caused by the reduction in the C29 alkane (Pighin *et al.*, 2004), we wanted to know if wax loads would be even further reduced in plants lacking both ABC transporters. *wbc11-3 cer5-2* double mutants were obtained by crossing *wbc11-3*/*WBC11* heterozygotes with the *cer5-2* knock-out mutant. Surprisingly, the total wax load of the double mutants, the genotypes of which were confirmed by PCR, did not show any significant difference in total wax load compared with *wbc11-3* (Table 1). Moreover, the contribution of individual compounds to the surface wax of *wbc11-3 cer5-2* was comparable with that of *wbc11-3* (Figure 5).

The presence of fusions in all *wbc11* mutants, which have been correlated with defects in cutin, led us to examine if *wbc11* lines had a reduction of cutin monomers in the stem compared with wild type. Strikingly, a strong 65% decrease in total cutin monomers was found in the knock-out allele *wbc11-3* (1.14 μg $cm^{-1} \pm 0.41$ SE) compared with wild type (3.29 μg $cm^{-1} \pm 0.07$ SE), which was not detected in the *cer5-2* mutant (3.74 μg $cm^{-1} \pm 0.14$ SE). This reduction was reflected in a 35–70% reduction of almost all individual cutin monomers extracted, including the most predominant

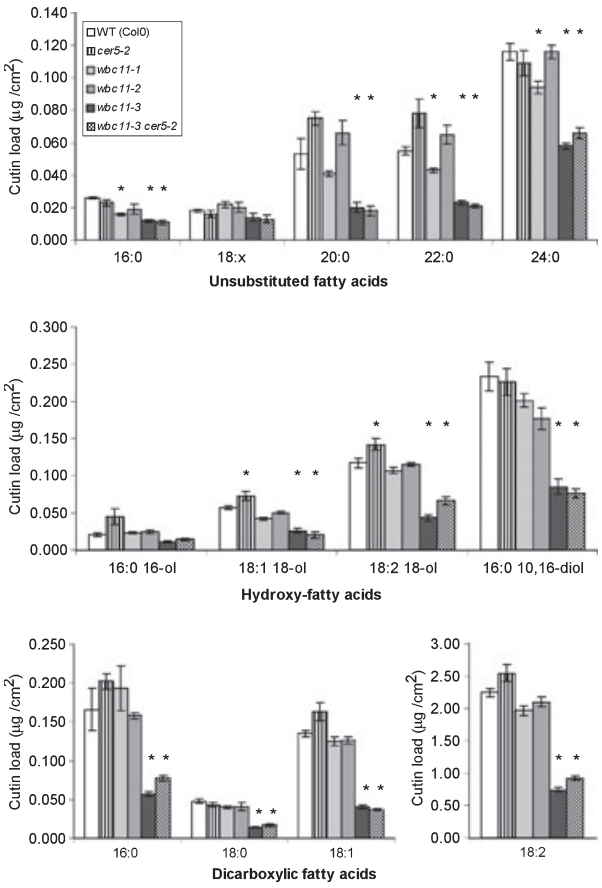

Figure 6. Cutin load is reduced in stems of *wbc11-3* mutants. Whole stems were analyzed for aliphatic monomers of lipid polyesters. The loads are expressed in μg per cm^2 of stem surface. *Means significantly different from wild type ($P < 0.05$). Values are means of six replicates. Error bars = SE.

monomer, C18:2 dicarboxylic acid (Figure 6). Some of the unsubstituted C16-C18 fatty acid monomers, which did not exhibit a strong decrease, are likely to be mostly arising from residual soluble lipids. Interestingly, almost all cutin monomer levels in the knock-down alleles *wbc11-1* and *wbc11-2*, which both displayed extensive stem–leaf fusions but no stunted growth phenotype, were not significantly lower than in wild type; the only exceptions being a small reduction of C22 and C24 fatty acid monomers in *wbc11-1* (Figure 6).

Alterations in epidermal cell ultrastructure in wbc11 *mutants*

Because of the homology of *WBC11* and *CER5* genes (76% similar, 54% identical at the amino acid level), we examined the epidermal cell ultrastructure of *wbc11-3* to determine if it, like *cer5-1*, had lipidic inclusions in the cytoplasm (Pighin *et al.*, 2004). In wild-type epidermal cells, the large central vacuole, surrounded by a thin layer of cortical cytoplasm and plasma membrane, dominated the epidermal cells (Figure 7a). Inside the stem epidermal cells of *wbc11* mutants, inclusions were observed in the cytoplasm that

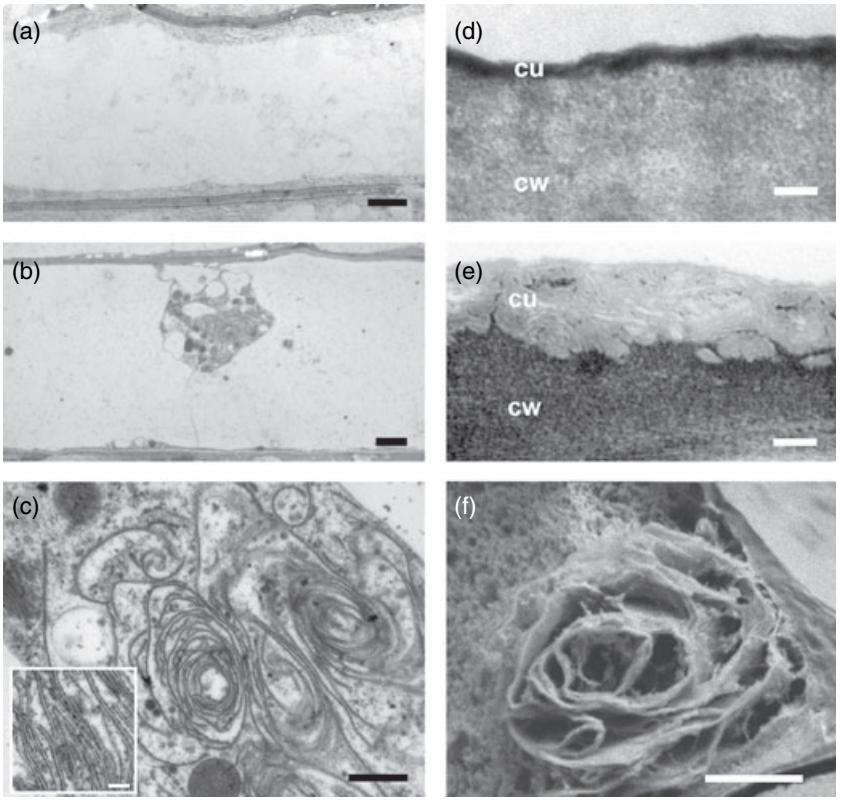

Figure 7. *wbc11-3* plants have a disorganized cuticle and contain electron-dense trilamellar inclusions in stem epidermal cells. Transmission electron micrographs (a–e), and a micrograph of a fractured *wbc11-3* stem using cryo-scanning EM (f).
(a) Tangential longitudinal section through wild-type stem epidermal cells.
(b) Tangential longitudinal section through *wbc11-3* epidermal stem cells with cytoplasm containing inclusions bulging into the central vacuole.
(c) High magnification of *wbc11-3* stem epidermal cells shown in (b), with trilamellar inclusions (inset).
(d) Transverse section of a wild-type stem epidermal cell showing the outermost periclinal cell wall and cuticle.
(e) Transverse section of *wbc11-3* stem showing a disorganized region of the cuticle.
(f) Cryo-scanning EM of fractured *wbc11-3* epidermal stem cells showing inclusions with a sheet-like morphology. Bars = 2 μm for (a) and (b), 500 nm for (c) and 100 nm in inset, 100 nm for (d) and (e) and 250 nm for (f). Abbreviations: cu, cuticle; cw, cell wall.

created large cytoplasmic protrusions into the central vacuole (Figure 7b). Examination of the inclusions at higher magnification revealed that they tended to aggregate into dense coils of trilamellar (dark-light-dark) ribbons (Figure 7c and inset). When *wbc11-3* stems were frozen, then fractured transversely and observed in cryo-SEM, inclusions appeared as concentric aggregated sheets within the cytoplasm, which correlated with the structures observed in thin sections (Figure 7f cf. Figure 7c).

In addition to the accumulation of cytoplasmic inclusions, *wbc11-3* plants showed dramatically altered cuticle morphology. Transverse sections of wild-type stems showed the thin (<100 nm), continuous electron-dense cuticle (Figure 7d). However, *wbc11-3* stems had numerous regions where the cuticle appeared to be more diffuse, disorganized, and only lightly stained (Figure 7e).

Yellow fluorescent protein-WBC11 fusion protein complements wbc11-3 *defects and is localized to the plasma membrane*

To confirm that the defects in growth, cuticle structure, and cuticular lipid levels in the *wbc11* mutants were all caused by disruptions in the *WBC11* gene, we expressed the cDNA of the gene as a YFP fusion in the knock-out mutant *wbc11-3* plants, under the control of the 35S promoter. Twelve independent transgenic lines were recovered, eleven of which had wild-type growth habit and fertility suggesting that the defects in the mutant were restored. When *wbc11-3* plants expressing YFP-WBC11 were analyzed for wax load, the levels observed were not significantly different from wild-type levels, but were significantly higher than in *wbc11-3* plants (Figure 8a). In all isolated transgenic lines, YFP fluorescence was observed in the periphery of the cells and was coincident with the plasma membrane (PM) stain, FM4-64 (Bolte *et al.*, 2004; Figure 8b–d). When the signal from the YFP-WBC was merged with the PM label from FM4-64, the signals co-localize, as seen in the inset in Figure 8d. When the YFP-WBC11 expressing stems were observed with a propidium iodide counter-stain, a membrane-impermeable dye which stains the cell wall (Figure 8d,e–g), the YFP fluorescence appeared directly appressed to the stained cell wall (Figure 8g, inset). To further confirm the YFP-WBC11 localization to the plasma membrane, we compared seedlings expressing YFP-WBC11 with seedlings expressing a tonoplast-localized GFP-δ-TIP (At3g16240; Cutler *et al.*, 2000). GFP-δ-TIP was found localized to small vacuoles in addition to the periphery of the cells, but was not co-localized with the FM4-64-labeled PM (Figure S1a–c).

Expression of WBC11 *in Arabidopsis*

To characterize the expression patterns of *WBC11*, a 2.6-kb fragment, upstream of the predicted translation start site of

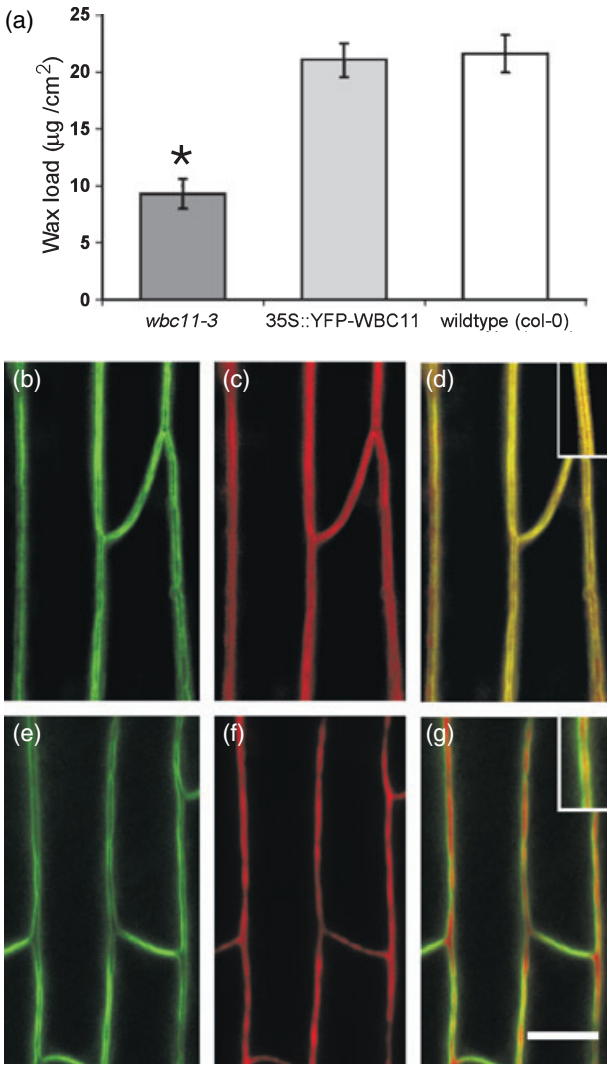

Figure 8. YFP-WBC11 is localized in the epidermal cell plasma membrane and complements the *wbc11-3* phenotype.
(a) *wbc11-3* plants expressing YFP-WBC11 show a normal stem wax load compared with wild type. Each value is the mean of five independent measurements of individual plants. *Means significantly different from wild type (ANOVA $F_{(2,15)} = 52.045$, $P < 0.001$; Tukey's HSD, $P < 0.05$). Error bars = SE.
(b–g) Confocal micrographs of *wbc11-3* stems expressing YFP-WBC11 fusion protein under the constitutive 35S promoter. (b, e) YFP-WBC11 is localized to the periphery of stem epidermal cells (green). (c) FM4-64 staining of plasma membranes (red). (d) Overlay of (b) and (c). (f) Propidium iodide (PI) stains cell walls (red). (g) Overlay of (e) and (f). The YFP-WBC11 signal is coincident with FM4-64 but not with PI. Bar = 10 μm.

WBC11, was used as a promoter to drive the expression of GUS in transgenic Arabidopsis plants. GUS activity was detected throughout the shoot system, particularly in stems (Figure 9a). Transverse sections of stems demonstrated GUS activity not only in the epidermis, but also in the cortical cells (Figure 9b). Trichomes on both stems and leaves also showed significant levels of GUS staining (Figure 9c). In contrast to the stems, GUS activity in leaves was restricted to the epidermal layers (Figure 9e). Flower buds, prior to anthesis, showed staining in all whorls, but GUS activity was strongest in anthers (Figure 9f). Upon anthesis, expression in the floral whorls was markedly reduced, except in the carpel (Figure 9g). Expression in the carpel was retained after pollination and during expansion of the silique; in addition, strong staining was observed in developing seeds (Figure 9h). Dissection of these seeds revealed GUS activity predominantly in the endosperm, with additional GUS activity detected in the embryo protoderm (data not shown).

GUS expression was also detected in root tips and emerging secondary root tips, even as early as the initial cell divisions of the pericycle (Figure 9i,k–n). Longitudinal sections of root tips revealed that, as in the stem, the *WBC11* 5′-promoter conferred expression primarily in the epidermis (or protoderm) and outermost cortical cells, but also in the root cap (Figure 9j). To confirm the GUS expression patterns of *WBC11* in wild-type plants, we used real-time PCR. *WBC11* transcript was detected in all organs, but was strongest in aerial organs and seeds, consistent with the promoter-GUS findings (Figure 9o).

Discussion

This study identifies WBC11 as a key component of the cuticular lipid export pathway. We have characterized three Arabidopsis *wbc11* T-DNA insertion mutants, which either reduce or abolish *WBC11* transcript accumulation. The *wbc11* mutants had inflorescence stem cuticles deficient in both cutin and wax, disorganized cuticle structure, *fiddlehead*-type post-genital organ fusions, changes in the numbers and shapes of epicuticular wax crystals, as well as accumulations of lipidic inclusions within the cytoplasm. We have also confirmed the permeable cuticle mutation *pel1* to be an allele of the *WBC11*, providing further evidence to show that WBC11 is required for cuticle formation. Thus WBC11 is the second ABC transporter, besides CER5, involved in the export of cuticular lipids from the epidermal cells.

WBC11 expression was detected in the epidermal cells of stems and leaves, consistent with the role of this gene in the formation of the cuticle. Although *WBC11* transcript was detected in roots using real time PCR, they had the lowest level of expression of all organs tested. The expression in roots was restricted to root tips, specifically to the protoderm, root cap cells and lateral root primordia; expression of *WBC11* was not observed in mature, differentiated cells. The function of *WBC11* in developing root tips is not clear; however, other genes shown to be involved in cuticle formation are also expressed in roots, namely *FDH* (Lolle *et al.*, 1992; Pruitt *et al.*, 2000; Yephremov *et al.*, 1999), *LCR* (Wellesen *et al.*, 2001), *WAX2/YRE* (Chen *et al.*, 2003; Kurata *et al.*, 2003), *LACS2* (Schnurr *et al.*, 2004), *ACE/HTH* (Krolikowski *et al.*, 2003; Kurdyukov *et al.*, 2006a), *CER5* (Pighin

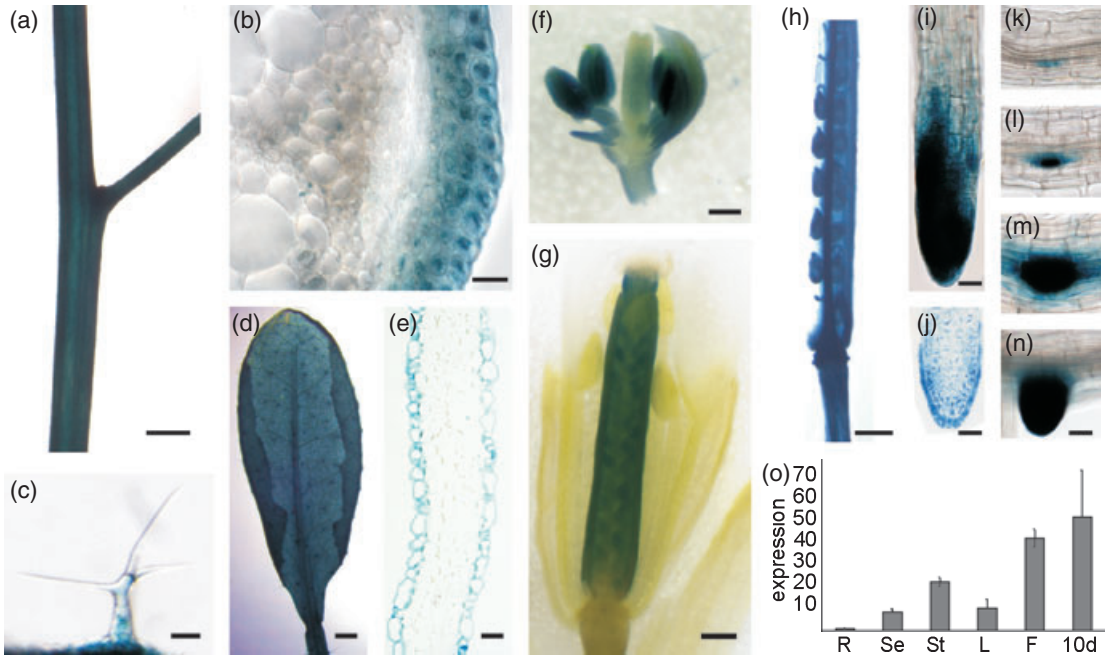

Figure 9. *WBC11* is expressed in aerial organs and root tips in Arabidopsis. Arabidopsis plants expressing GUS under control of the *WBC11* promoter (a–o). (a) Whole stem showing uniform GUS expression along the stem; bar = 0.5 mm. (b) Cross section of stem with expression in the epidermis and the chlorenchymous layers of the cortex; bar = 50 μm. (c) Leaf trichome; bar = 50 μm. (d) Rosette leaf; bar = 0.25 mm. (e) Leaf cross section with expression in the epidermal layers; bar = 25 μm. (f) Dissected floral bud. GUS is expressed in all whorls, but predominantly in anthers; bar = 100 μm. (g) Mature flower, post-anthesis. GUS is expressed in carpels, but is no longer detected in other whorls; bar = 250 μm. (h) Partly-dissected silique. GUS is expressed during elongation and maturation of the silique as well as developing seeds; bar = 0.5 mm. (i) Primary root tip; bar = 20 μm. (j) Longitudinal section of root tip. GUS is predominantly expressed in the root cap and the protoderm; bar = 20 μm. (k) GUS activity is detected within a single cell of the pericycle. (l–n) Developing lateral roots; bars = 25 μm. (o) Real-time PCR showing *WBC11* expression in different organs. Expression level is normalized to *ACTIN1* expression; R, root; Se, seedling; St, Stem; L, leaf; F, flower buds and flowers; 10d, 10-day-old (post-anthesis) seeds; bars represent SD (n = 4).

et al., 2004), *BDG* (Kurdyukov *et al.*, 2006b) and *CER4* (Rowland *et al.*, 2006).

There are four possible hypotheses for the combined cutin and wax deficiency in *wbc11*: (i) WBC11 is only indirectly involved in cuticle formation, and the cutin and wax alterations are effects of an unknown transport function of WBC11; (ii) WBC11 transports only wax, and the cutin phenotype is an indirect effect; (iii) WBC11 transports only cutin precursors, and the wax phenotype is an indirect effect; (iv) WBC11 transports both wax and cutin precursors. We find (i) unlikely, given the high degree of similarity of WBC11 to known lipid transporters such as CER5 (76% similarity) and human ABCG5 (47%) and ABCG8 (49%; Pighin *et al.*, 2004; Wang *et al.*, 2006). Therefore, the transport of lipids by WBC11 is consistent with conservation of function in this gene family. Assuming the simplest scenario, that cuticular lipids are substrates, this raises the question of whether the function of WBC11 is to transport cutin, wax or both.

WBC11 is required for normal cutin deposition

The *wbc11-3* plants exhibited a 65% reduction of cutin monomers. In contrast, the levels of cutin monomers in the knock-down alleles, *wbc11-1* and *-2*, were not significantly different from wild type, with the exception of only C22 and C24 unsubstituted fatty acids. This suggests that complete elimination of *WBC11* transcript was necessary to cause a significant drop in cutin deposition.

In addition to the reduction in extractable cutin monomers, *wbc11-3* plants had regions where the cuticle was more disorganized, more diffuse and electron-translucent. Similar disorganized regions of the cuticle have also been found in mutants with cuticle defects caused by alterations in cutin composition, including *wax2, bodyguard, lacs2* and *lacerata* (Chen *et al.*, 2003; Kurdyukov *et al.*, 2006b; Lolle *et al.*, 1992; Schnurr *et al.*, 2004; Wellesen *et al.*, 2001), and Arabidopsis plants overexpressing fungal cutinase (Sieber *et al.*, 2000).

The absence of WBC11 transporter also resulted in extensive post-genital stem–stem, stem–leaf and leaf–leaf fusions, which are often found in mutants with cutin-specific defects (Tanaka and Machida, 2006). Reduction in cutin content alone is not likely to be sufficient to cause organ fusions, because *att1* plants, which have 30% lower cutin monomer levels, were not reported to have organ fusions (Xiao *et al.*, 2004). On the other hand, some mutants with disorganized cuticles, but normal absolute levels of cutin,

such as *bodyguard* (Kurdyukov *et al.*, 2006b), exhibit post-genital fusions, suggesting that disorganization of cutin may be the key factor resulting in fusion of organs.

In addition to organ fusions found in all of the *wbc11* alleles, the knock-out *wbc11-3* mutant was dwarf and sterile. These latter defects are likely to be pleiotropic effects of the impaired cuticle. Reduced growth and fertility have been commonly observed in plants with cuticle defects including *ale1*, *lacerata*, *wax2, lacs2* and *bodyguard* (Chen *et al.*, 2003; Kurdyukov *et al.*, 2006b; Pighin *et al.*, 2004; Schnurr *et al.*, 2004; Tanaka *et al.*, 2001; Wellesen *et al.*, 2001). It is possible that wax transport defects of *wbc11-3* lead to infertility and dwarfism. However, mutants with wax loads comparable with *wbc11-3*, such as *cer5* (Pighin *et al.*, 2004), or more severely reduced wax loads, such as *cer6*, did not have changes in growth (Hooker *et al.*, 2002; Millar *et al.*, 1999).

Taken together, the disorganized cuticular layer, reduced levels of cutin monomers and organ fusions of *wbc11* mutants provide compelling evidence of the importance of this ABC transporter to the process of cutin formation.

WBC11 is required for wax transport

Similar to *cer5* mutants, *wbc11-3* had fewer epicuticular wax crystals than the wild type, suggesting a lower wax load. All T-DNA mutants of *WBC11* had a wax load that was 40–50% that of wild type. *wbc11-3* was further found to accumulate trilamellar inclusions in the stem epidermal cells, as observed in TEM, and lipidic sheets, as observed in cryo-SEM. Lipidic inclusions were also observed in *cer5-1*, which accumulated wax in the epidermal cells; thus, it seems likely that the inclusions in *wbc11-3* are the same in nature (Pighin *et al.*, 2004). Unfortunately, because of the strongly hydrophobic nature of the wax substrates, we cannot currently assay WBC11 transport activity biochemically. Nevertheless, these data strongly support the hypothesis that WBC11, like CER5, is directly involved in wax transport.

Interestingly, the wax load deficiency in *wbc11* alleles was largely the result of a 75–90% reduction in C29 alkane (nonacosane), the most abundant component of wild-type stem wax. Furthermore, nonacosane levels appeared to correlate with levels of *wbc11* transcript, which, if the transporter is moving wax molecules directly, indicates WBC11 shows a substrate preference for alkanes, and specifically nonacosane. In contrast to the alkanes, some wax components, such as the C29 secondary alcohols and C29 ketone, were not as much reduced in the *wbc11-3* knock-out as in with the *wbc11-1* and *-2* knock-down mutants. This result could represent a compensatory effect induced by the total loss of *WBC11* gene transcript, for example an increase in the biosynthesis and/or the transport of wax components other than nonacosane. This compensation does not appear to involve CER5 at the transcriptional level, as *CER5* expression was not changed in *wbc11* mutants compared with wild type. Furthermore, the *wbc11-3 cer5-2* double mutant had similar wax loads. It follows that other transporters, besides WBC11 and CER5, are involved in wax export on Arabidopsis stems. In support of this latter hypothesis, we note that other ABC transporters were also found up-regulated in the transcriptome of epidermal cells, as compared to neighbouring tissues (Suh *et al.*, 2005).

WBC11 may physically interact with CER5

Analysis of the *cer5* and *wbc11* mutants demonstrated identical strong reductions in the predominant wax component for Arabidopsis stems, nonacosane, and accumulation of intracellular lipidic inclusions. Therefore, these two ABC transporters may have similar, but separate, roles in wax export. If this is the case, then mutations in both genes in the *wbc11-3 cer5-2* double mutant should show an additive effect, and result in a lower wax load than that found in either single mutant. In contrast to this prediction, the cuticular lipid analysis of the double mutant revealed that there was no difference in wax load between the single *wbc11-3* and *cer5-2* mutants and the corresponding *wbc11-3 cer5-2* double mutant. These results indicate that both *WBC11* and *CER5* gene products act in the same pathway or complex. As the ABCG/WBC subfamily of ABC transporters are 'half-transporters', and require dimerization to be functional, it is conceivable that CER5 and WBC11 form heterodimers that function in the export of waxes, particularly nonacosane. Protein–protein interaction studies are currently underway to test this hypothesis directly.

Can WBC11 transport both cutin precursors and wax?

Our results provide evidence that WBC11 is involved in export of both cutin precursors and wax. At this point, however, it cannot be ruled out that WBC11 is specific for only one of these cuticle lipid classes, and the loss of function has a secondary, indirect effect on the accumulation of the other component. Such an indirect effect could be mediated by altered physicochemical properties of the mutant wax, which in turn disrupt cutin assembly, or by altered transport of a wax component playing a signaling role for cutin biogenesis. However, it appears unlikely that WBC11 is directly involved in wax transport only, because mutations in *CER5*, which result in a similar reduction of wax load as *wbc11* mutations, show neither a decrease in cutin monomers nor any cutin defects. An extreme hypothesis would be that cutin deposition is influenced mostly by very low abundance wax compounds, which thus may play a kind of signaling role in cuticle biogenesis (Lolle and Pruitt, 1999). However,

there is no experimental evidence that such a signaling pathway exists in the extracellular matrix.

It also seems unlikely that WBC11 is directly involved in cutin transport only. There is little evidence in the literature to suggest that cutin defects are coupled with loss of wax. On the contrary, mutants with altered cutin (including *bodyguard* and *lacs2*) as well as cutinase overexpressing plants do not show any detrimental effect on wax load, but instead have higher wax loads (Kurdyukov *et al.*, 2006b; Schnurr *et al.*, 2004; Sieber *et al.*, 2000). Although other mechanisms cannot be ruled out, the simplest hypothesis is that WBC11 is directly involved in both cutin precursor and wax transport. If WBC11 is involved in transporting cutin precursors, then we must assume that assembly of the cutin polyester is extracellular. Thus the exported cutin precursors could be, for example, in the form of oligomers, acylglycerols or free fatty acids.

This raises the question of how this protein could transport substrates as diverse as these two classes of lipids. Arabidopsis cutin is rich in 18:2 and 16:0 dicarboxylates and a variety of C16 and C18 hydroxy-fatty acids (Bonaventure *et al.*, 2004; Franke *et al.*, 2005). In contrast, the wax components have much longer aliphatic chains, fully saturated carbon backbones and typically only one functional group. Many ABC transporters are capable of accepting a wide range in substrates (Chang, 2003). For example, a human orthologue of Arabidopsis WBC11, ABCG2/BRCP is capable of transporting a diverse array of hydrophobic xenobiotics (Xu *et al.*, 2004). Still, despite the substrate promiscuity of ABC transporters, it is difficult to explain how WBC11 would discriminate between fairly similar wax molecules, such as nonacosane and the oxygenated C29 molecules, and at the same time be capable of transporting the structurally different cutin precursors.

However, we must keep in mind that WBC11 is a half-transporter, and thus may represent only one-half of one or more full-transporters composed of itself and another WBC family member. Such is the case with the *Drosophila WHITE*, *BROWN* and *SCARLET* gene products, where WHITE pairs with BROWN or SCARLET to form two different transporters to transport tryptophan- or guanine- derivatives, respectively (Dreesen *et al.*, 1988). Thus, we propose a model where WBC11 forms different dimers to export wax or cutin precursors. Specifically, WBC11 and CER5 may form a heterodimer that functions in the transport of wax, particularly C29 alkane, whereas WBC11 may partner with itself to form a homodimer, or with an unidentified ABCG/WBC transporter, for the transport of cutin precursors. If WBC11 does have function in multiple interactions as described, then it is likely to have a higher affinity to form the cutin-transporting dimer, as the cutin monomer levels were reduced in the knock-out *wbc11-3*, but not in the knock-downs, *wbc11-1* and *-2*.

Conclusions

In summary, we have characterized the Arabidopsis WBC11 transporter using a reverse genetics approach, and have demonstrated that it is required for the accumulation of both cutin and wax. We have further shown that WBC11 is localized to the plasma membrane where it may interact with CER5. These findings lead to interesting testable hypotheses, including: (i) heterodimers between CER5 and WBC11 transport wax; and (ii) WBC11 homodimers, or heterodimers with an unknown partner, are required for cutin accumulation.

Experimental procedures

Plant material and growth conditions

Arabidopsis thaliana seeds were stratified for 3–4 days at 4°C, and plants were grown on a mixture of sunshine mix 5 (Sun Gro Horticulture Inc., http://www.sungro.com) under white fluorescent light (80–100 $\mu E\ m^{-2}\ sec^{-1}$) in a constant photoperiod at 21°C. Salk T-DNA insertional mutant lines were obtained from the Arabidopsis Biological Resource Centre (http://www.arabidopsis.org). Seeds of the *pel1-1* mutant were a gift to AY received from Prof. Y. Machida (Nagoya University).

Stem harvest and surface area measurements

Primary stems were harvested from 5–6-week-old plants. After removal of the cauline leaves and siliques, stems were photographed with a digital camera. Surface areas were calculated by measuring the area of the two-dimensional projection of the stem, assuming a cylindrical geometry.

Cryo-scanning electron microscopy

Segments from the apical 4–6 cm of stem were mounted onto cryo-SEM stubs using graphite paste and plunged into liquid nitrogen. Frozen stems were transferred into an Emitech K1250 cryo-system, where stems were fractured and water sublimed for 10 min at −110°C. Samples were viewed with a Hitachi S4700 field emission SEM (Nissei Sangyo America Ltd.; http://www.hitachi.us) using an accelerating voltage of 1.5 kV and a working distance of 12 mm.

High-pressure freezing and transmission electron microscopy

Segments (1–2 mm thick) from the apical 0.5–1 cm of the bolting stem or basal leaves were high-pressure frozen, freeze-substituted and embedded in Spurr's resin as previously described by Rensing *et al.* (2002). Briefly, stem and leaf segments were cut in 0.2 M sucrose and subsequently high-pressure frozen in a Balzers HPM 010 (Bal-tec AG; http://www.bal-tec.com). Frozen samples were freeze-substituted for 5 days in 2% osmium tetroxide and 8% dimethoxypropane in acetone using a dry ice–acetone bath. Tissues were then warmed to −20°C for 4 h, to 4°C for 4 h and to room temperature for a final 4 h. Tissues were rinsed in fresh acetone and gradually infiltrated and embedded with Spurr's resin. Embedded tissues were

sectioned at 70 nm and mounted onto uncoated 300-mesh hexagonal grids, stained with 2% uranyl acetate in 70% methanol for 20 min and Reynold's lead citrate for 10 min. Digital images were captured with a Hitachi 7600 (Nissei Sangyo America Ltd.) at 80 kV.

Laser-scanning confocal microscopy

Stem sections from 5-week-old plants or hypocotyls from 5-day-old seedlings were mounted in distilled water and observed on a Zeiss LSM 510 Meta laser scanning microscope (Carl Zeiss Inc., http://www.zeiss.com). GFP fluorescence was detected using excitation of 488 nm with a 505–530-nm band-pass filter. YFP fluorescence was detected using excitation of 514 nm with a 535–580-nm band-pass filter. For cell wall staining, tissue was immersed in 1 μg ml^{-1} propidium iodide solution prior to mounting. For plasma membrane staining, tissues were immersed in FM4-64 solution (10 μM) for 10 min. Propidium idodide and FM4-64 staining was detected using an excitation of 514 nm with a 600–650-nm band-pass filter. Images were processed with LSM 5 Image Browser (Carl Zeiss Inc.) and Corel Photopaint 8.0 software (Corel, http://www.corel.com).

Wax analysis

The cuticular waxes were extracted by immersing whole inflorescence stems or 10-cm-long segments of stems two times for 30 sec into 5–10 ml of chloroform ($CHCl_3$) at 21°C. Both $CHCl_3$ solutions were combined and n-tetracosane was added as the internal standard. The solvent was removed under a gentle stream of nitrogen gas, and the remaining wax mixture was re-dissolved in 1 ml of $CHCl_3$ and stored at 4°C until used. Prior to GC analysis, chloroform was evaporated from the samples under a gentle stream of nitrogen gas while heating to 50°C. Then the wax mixtures were treated with bis-*N*,*N*-(trimethylsilyl) trifluoroacetamide (BSTFA; Sigma, http://www.sigmaaldrich.com) in pyridine (30 min at 70°C) to transform all hydroxyl-containing compounds into the corresponding trimethylsilyl derivatives. The qualitative composition was studied with capillary GC (Agilent 5890 N, http://www.agilent.com; column 30 m Hewlett-Packard-1, 0.32-mm inner diameter, film thickness 0.1 mm; http://welcome.hp.com/country/us/en/wwwelcome.html) with an He carrier gas inlet pressure regulated for a constant flow of 1.4 ml min^{-1} and an MS detector (Agilent 5973 N). GC was carried out with temperature-programmed injection in a 50°C oven, 2 min at 50°C, raised by 40°C min^{-1} to 200°C, held for 2 min at 200°C, raised by 3°C min^{-1} to 320°C, and held for 30 min at 320°C. The quantitative composition of the mixtures was studied using capillary GC with FID under the same GC conditions as above, but H_2 carrier gas inlet pressure was regulated for constant flow of 2 ml min^{-1}. Single compounds were quantified against the internal standard by automatically integrating peak areas.

Polyester analysis

Surface waxes of whole stems from 6–8-week-old plants were first extracted as described above. Stems were then immediately processed to extract and quantify lipid polyesters according to the method described by Bonaventure *et al.* (2004) with the slight modifications described in Suh *et al.* (2005). Briefly, after extensive delipidation of the ground stems, the resulting dry residue was depolymerized using the sodium methoxide method. Polyester monomers were separated, identified and quantified by GC-MS. Splitless injection was used and the mass spectrometer run in scan mode over 40–500 amu (electron impact ionization), with peaks quantified on the basis of their total ion current. Polyester monomer quantities were expressed per unit of surface area, which was determined as indicated for waxes. The initial wax extractions were used to verify the wax loads.

Statistical analysis

Data analysis was conducted with SYSTAT 12 software (Systat Software, http://www.systat.com). When assumptions of normalcy and homoscedasticity were met, significance was analyzed using ANOVA and Tukey's honestly significant differences (HSD) post-hoc tests. In cases of heterogeneous variance, the Games–Howell multiple comparisons test was used to analyze significance (Sokal and Rohlf, 1995).

Transgene constructs and plant transformation

The native WBC11 promoter was amplified from genomic DNA using gene specific primers (forward primer 5′-GGGGACAAGTTTGTACAAAAAAGCAGGCTATGGTGAACTCCGGCCATAGAAAC-3′; reverse primer 5′-GGGGACCACTTTGTACAAGAAAGCTGGGTGTCTAGACTCTTAAACCAAAAC-3′) and the PCR product was cloned into pDONR 221 using BP Clonase (Invitrogen, http://www.invitrogen.com) to create pD-WBC11pro. Following this, the WBC11 promoter cassette was transferred to pGWB3 (T. Nakagawa, unpublished data) using LR Clonase (Invitrogen) to create pWBC11pro::GUS and was confirmed by sequencing. The WBC11 open reading frame (ORF) was amplified from wild-type cDNA using gene-specific primers (forward primer 5′-GGGGACAAGTTTGTACAAAAAAGCAGGCTCCATGGAGATAGAAGCAAGCAGACAAC-3′; reverse primer 5′-GGGGACCACTTTGTACAAGAAAGCTGGGTCTACCATCTGCGAGCTCC-3′) and the PCR product was cloned into pDONR 221 using BP Clonase (Invitrogen) to create pD-WBC11. Following this, the WBC11 ORF was transferred to pEARLEYGATE 104 (Earley *et al.*, 2006) to create an *N*-terminal YFP-fusion to WBC11 using the CaMV 35S promoter for constitutive expression in plants. Arabidopsis plants (wild-type Col-0, and heterozygotes *wbc11-3/WBC11*) were transformed using the floral dip method (Clough and Bent, 1998).

Gene expression analysis

Total RNA was extracted from whole-stem segments using TRIzol reagent (Invitrogen). Double-stranded cDNA was synthesized from approximately 15 mg of total RNA by using a double-stranded cDNA synthesis kit (Fermentas, http://www.fermentas.com) with oligo-d(T) primer. A 2-μl sample of a 20-μl reaction (approximately 3 μg of cDNA) was used for semi-quantitative RT-PCR reactions with gene-specific primers for At1g17840 (forward primer 5′-ATGGAGATAGAAGCAAGC-3′; reverse primer 5′-CCATCTGCGGGCTCCATC-3′), At1g51500 (forward primer 5′-ATGGAGTTAGAGAGTACG-3′; reverse primer 5′-ATTAATTGGAGAGGTAAGACC-3′), At5g53300 (forward primer 5′-GATCTTTGCCGGAAAACAATTGGAGGATGGT-3′; reverse primer 5′-CGACTTGTCATTAGAAAGAAAGAGATAACAGG-3′). The PCR reaction was performed in an MJ Research PTC 200 thermocycler (Waltham, MA, USA) using Hot Start Taq (Fermentas) with the following conditions: initial denaturation 95°C for 4 min, followed by twenty cycles of 95°C for 30 sec, 55°C for 45 sec, 72°C for 120 sec and a final 10-min extension at 72°C. Quantitative Real-time PCR was performed using SYBR Green to monitor dnDNA synthesis using a Bio-Rad miniOpticon real-time PCR detection system (Bio-Rad, http://www.bio-rad.com) according to the manufacturer's directions. RNA levels were normalized using *ACTIN2* (At3g18780) as a housekeeping gene. Efficiencies were calculated

using a 10-fold serial dilution series of DNA. Primers for *WBC11* (forward primer 5′-GCCGCAAAACCAAACTCTCCTTTG-3′; reverse primer 5′-CTTCTCTCCACCACTAATTCCACGC-3′) and *ACT2* (forward primer 5′-CCAGAAGGATGCATATGTTGGTGA-3′; reverse primer 5′-GAGGAGCCTCGGTAAGAAGA-3′) were used. Reaction conditions were as follows: initial denaturation 95°C for 2 min, followed by forty cycles of 95°C for 20 sec, 55°C for 10 sec, 72°C for 10 sec and a final 5-min extension at 72°C. A dissociation analysis was conducted in order to check for the specificity of primers to the genes of interest. Results were analyzed using the Bio-Rad OPTICON MONITOR 3 software (Bio-Rad).

GUS expression analysis

Expression of GUS in transgenic WBC11promoter::GUS plants (wild-type Col-0 background) was assayed as described (Koizumi *et al.*, 2000) with the modification of a 4-h incubation at 37°C. Stained seedlings were mounted directly in water. Alternatively, tissue specimens were processed using microwave embedding into Spurr's resin. Sections (2-μm thick) were cut on a Leica Ultracut microtome (http://www.leica.com), mounted on glass slides and imaged using a QCAM digital camera (QImaging, http://www.qimaging.com) and OPENLAB 4.01 (Improvision, http://www.improvision.com).

Acknowledgements

We thank the Salk Institute for Genomic Analysis Laboratory for providing sequence-indexed Arabidopsis T-DNA insertion mutants *wbc11-1* (SALK_144827), *wbc11-2* (SALK_112720) and *wbc11-3* (SALK_119873). We are grateful to Prof. Y. Machida (Nagoya University) for providing *pel1-1* and *-2* seeds to AY. We thank Tsuyoshi Nakagawa for the pGWB3 vector. We thank the Bio-imaging Facility at the University of British Columbia for providing microscopy support. We are grateful to Graeme Bell for technical assistance. We thank Allan DeBono and Miao Wen for thoughtful discussion and comments on the manuscript. GABI-KAT T-DNA mutants were generated in the context of the GABI-Kat program and were provided by Bernd Weisshaar (MPI for Plant Breeding Research; Cologne, Germany). We thank M. Pollard and J. Ohrogge for careful review and comments on the manuscript. Thanks also to Eric Johnson for technical and editorial assistance and L.R. Linton for advice on statistical analysis. ALS, LK and RJ gratefully acknowledge funding from an NSERC Special Research Opportunity Grant in support of this work.

Supplementary Material

The following supplementary material is available for this article online:

Figure S1. Stem epidermal wax load is restored in *wbc11* plants expressing *35S::YFP-WBC11.*

Figure S2. Comparison of YFP-WBC11 and tonoplast-localized δ-TIP-GFP.

This material is available as part of the online article from http://www.blackwell-synergy.com

References

Alonso, J.M., Stepanova, A.N., Leisse, T.J. *et al.* (2003) Genome-wide insertional mutagenesis of *Arabidopsis thaliana*. *Science*, **301**, 653–657.

Bolte, S., Talbot, C., Boutte, Y., Catrice, O., Read, N.D. and Satiat-Jeunemaitre, B. (2004) FM-dyes as experimental probes for dissecting vesicle trafficking in living plant cells. *J. Microsc. Oxford*, **214**, 159–173.

Bonaventure, G., Beisson, F., Ohlrogge, J. and Pollard, M. (2004) Analysis of the aliphatic monomer composition of polyesters associated with Arabidopsis epidermis: occurrence of octadeca-cis-6, cis-9-diene-1,18-dioate as the major component. *Plant J.* **40**, 920–930.

Browse, J. and Somerville, C. (1991) Glycerolipid synthesis – biochemistry and regulation. *Annu. Rev. Plant Physiol.* **42**, 467–506.

Chang, G. (2003) Multidrug resistance ABC transporters. *FEBS Lett.* **555**, 102–105.

Chen, X.B., Goodwin, S.M., Boroff, V.L., Liu, X.L. and Jenks, M.A. (2003) Cloning and characterization of the *WAX2* gene of Arabidopsis involved in cuticle membrane and wax production. *Plant Cell*, **15**, 1170–1185.

Clough, S.J. and Bent, A.F. (1998) Floral dip: a simplified method for *Agrobacterium*-mediated transformation of *Arabidopsis thaliana*. *Plant J.* **16**, 735–743.

Cutler, S.R., Ehrhardt, D.W., Griffitts, J.S. and Somerville, C.R. (2000) Random GFP::cDNA fusions enable visualization of subcellular structures in cells of Arabidopsis at a high frequency. *Proc. Natl Acad. Sci. USA*, **97**, 3718–3723.

Dreesen, T.D., Johnson, D.H. and Henikoff, S. (1988) The brown protein of *Drosophila melanogaster* is similar to the white protein and to components of active-transport complexes. *Mol. Cell. Biol.* **8**, 5206–5215.

Earley, K.W., Haag, J.R., Pontes, O., Opper, K., Juehne, T., Song, K. and Pikaard, C.S. (2006) Gateway-compatible vectors for plant functional genomics and proteomics. *Plant J.* **45**, 616–629.

Ewart, G.D., Cannell, D., Cox, G.B. and Howells, A.J. (1994) Mutational analysis of the traffic Atpase (Abc) transporters involved in uptake of eye pigment precursors in *Drosophila melanogaster* – implications for structure–function relationships. *J. Biol. Chem.* **269**, 10370–10377.

Franke, R., Briesen, I., Wojciechowski, T., Faust, A., Yephremov, A., Nawrath, C. and Schreiber, L. (2005) Apoplastic polyesters in Arabidopsis surface tissues – a typical suberin and a particular cutin. *Phytochemistry*, **66**, 2643–2658.

Graça, J., Schreiber, L., Rodrigues, J. and Pereira, H. (2002) Glycerol and glyceryl esters of omega-hydroxyacids in cutins. *Phytochemistry*, **61**, 205–215.

Hooker, T.S., Millar, A.A. and Kunst, L. (2002) Significance of the expression of the CER6 condensing enzyme for cuticular wax production in Arabidopsis. *Plant Physiol.* **129**, 1568–1580.

Jetter, R., Schaffer, S. and Riederer, M. (2000) Leaf cuticular waxes are arranged in chemically and mechanically distinct layers: evidence from *Prunus laurocerasus* L. *Plant Cell Environ.* **23**, 619–628.

Jetter, R., Kunst, L. and Samuels, A.L. (2006) Composition of plant cuticular waxes. In *Biology of the Plant Cuticle* (Riederer, M. and Müller, C., eds). Ames, IA: Blackwell Publishing, pp. 145–181.

Koizumi, K., Sugiyama, M. and Fukuda, H. (2000) A series of novel mutants of *Arabidopsis thaliana* that are defective in the formation of continuous vascular network: calling the auxin signal flow canalization hypothesis into question. *Development*, **127**, 3197–3204.

Kolattukudy, P.E. (1984) Biochemistry and function of cutin and suberin. *Can. J. Bot.* **62**, 2918–2933.

Krolikowski, K.A., Victor, J.L., Wagler, T.N., Lolle, S.J. and Pruitt, R.E. (2003) Isolation and characterization of the Arabidopsis organ fusion gene *HOTHEAD*. *Plant J.* **35**, 501–511.

Kunst, L. and Samuels, A.L. (2003) Biosynthesis and secretion of plant cuticular wax. *Prog. Lipid Res.* **42**, 51–80.

Kurata, T., Kawabata-Awai, C., Sakuradani, E., Shimizu, S., Okada, K. and Wada, T. (2003) The *YORE-YORE* gene regulates multiple aspects of epidermal cell differentiation in Arabidopsis. *Plant J.* **36**, 55–66.

Kurdyukov, S., Faust, A., Trenkamp, S., Bar, S., Franke, R., Efremova, N., Tietjen, K., Schreiber, L., Saedler, H. and Yephremov, A. (2006a) Genetic and biochemical evidence for involvement of HOTHEAD in the biosynthesis of long-chain alpha-,omega-dicarboxylic fatty acids and formation of extracellular matrix. *Planta*, **224**, 315–329.

Kurdyukov, S., Faust, A., Nawrath, C. *et al.* (2006b) The epidermis-specific extracellular BODYGUARD controls cuticle development and morphogenesis in Arabidopsis. *Plant Cell*, **18**, 321–339.

Lolle, S.J. and Pruitt, R.E. (1999) Epidermal cell interactions: a case for local talk. *Trends Plant Sci.* **4**, 14–20.

Lolle, S.J., Cheung, A.Y. and Sussex, I.M. (1992) Fiddlehead – an Arabidopsis mutant constitutively expressing an organ fusion program that involves interactions between epidermal cells. *Dev. Biol.* **152**, 383–392.

Millar, A.A., Clemens, S., Zachgo, S., Giblin, E.M., Taylor, D.C. and Kunst, L. (1999) CUT1, an Arabidopsis gene required for cuticular wax biosynthesis and pollen fertility, encodes a very-long-chain fatty acid condensing enzyme. *Plant Cell*, **11**, 825–838.

Nawrath, C. (2002) The biopolymers cutin and suberin. In *The Arabidopsis Book* (Somerville, C. and Meyerowitz, E.M. eds) Rockville, MD: American Society of Plant Biologists, doi: 10.1199/tab.0021.

Nawrath, C. (2006) Unraveling the complex network of cuticular structure and function. *Curr. Opin. Plant Biol.* **9**, 281–287.

Neinhuis, C. and Barthlott, W. (1997) Characterization and distribution of water-repellent, self-cleaning plant surfaces. *Ann. Bot.* **79**, 667–677.

Pighin, J.A., Zheng, H.Q., Balakshin, L.J., Goodman, I.P., Western, T.L., Jetter, R., Kunst, L. and Samuels, A.L. (2004) Plant cuticular lipid export requires an ABC transporter. *Science*, **306**, 702–704.

Pruitt, R.E., Vielle-Calzada, J.P., Ploense, S.E., Grossniklaus, U. and Lolle, S.J. (2000) *FIDDLEHEAD,* a gene required to suppress epidermal cell interactions in Arabidopsis, encodes a putative lipid biosynthetic enzyme. *Proc. Natl Acad. Sci. USA*, **97**, 1311–1316.

Rensing, K.H., Samuels, A.L. and Savidge, R.A. (2002) Ultrastructure of vascular cambial cell cytokinesis in pine seedlings preserved by cryofixation and substitution. *Protoplasma*, **220**, 39–49.

Rosso, M.G., Li, Y., Strizhov, N., Reiss, B., Dekker, K. and Weisshaar, B. (2003) An *Arabidopsis thaliana* T-DNA mutagenized population (GABI-Kat) for flanking sequence tag-based reverse genetics. *Plant Mol. Biol.* **53**, 247–259.

Rowland, O., Zheng, H., Hepworth, S.R., Lam, P., Jetter, R. and Kunst, L. (2006) *CER4* encodes an alcohol-forming fatty acyl-coenzyme A reductase involved in cuticular wax production in Arabidopsis. *Plant Physiol.* **142**, 866–877.

Sanchez-Fernandez, R., Davies, T.G.E., Coleman, J.O.D. and Rea, P.A. (2001) The *Arabidopsis thaliana* ABC protein superfamily, a complete inventory. *J. Biol. Chem.* **276**, 30231–30244.

Schnurr, J., Shockey, J. and Browse, J. (2004) The acyl-CoA synthetase encoded by LACS2 is essential for normal cuticle development in Arabidopsis. *Plant Cell*, **16**, 629–642.

Sieber, P., Schorderet, M., Ryser, U., Buchala, A., Kolattukudy, P., Metraux, J.-P. and Nawrath, C. (2000) Transgenic Arabidopsis plants expressing a fungal cutinase show alterations in the structure and properties of the cuticle and postgenital organ fusions. *Plant Cell*, **12**, 721–738.

Sokal, R.R. and Rohlf, F.J. (1995) *Biometry*. New York: W H Freeman and Company.

Stark, R.E. and Tian, S. (2006) The cutin biopolymer matrix. In *Biology of the Plant Cuticle* (Riederer, M. and Müller, C., eds). Ames, IA: Blackwell Publishing, pp. 126–144.

Suh, M.C., Samuels, A.L., Jetter, R., Kunst, L., Pollard, M., Ohlrogge, J. and Beisson, F. (2005) Cuticular lipid composition, surface structure, and gene expression in Arabidopsis stem epidermis. *Plant Physiol.* **139**, 1649–1665.

Tanaka, H. and Machida, Y. (2006) The cuticle and cellular interactions. In *Biology of the Plant Cuticle* (Riederer, M. and Müller, C., eds). Ames, IA: Blackwell Publishing, pp. 312–333.

Tanaka, H., Onouchi, H., Kondo, M., Hara-Nishimura, I., Nishimura, M., Machida, C. and Machida, Y. (2001) A subtilisin-like serine protease is required for epidermal surface formation in Arabidopsis embryos and juvenile plants. *Development*, **128**, 4681–4689.

Tanaka, T., Tanaka, H., Machida, C., Watanabe, M. and Machida, Y. (2004) A new method for rapid visualization of defects in leaf cuticle reveals five intrinsic patterns of surface defects in Arabidopsis. *Plant J.* **37**, 139–146.

Wang, J., Sun, F., Zhang, D.W., Ma, Y.M., Xu, F., Belani, J.D., Cohen, J.C., Hobbs, H.H. and Xie, X.S. (2006) Sterol transfer by ABCG5 and ABCG8 – in vitro assay and reconstitution. *J. Biol. Chem.* **281**, 27894–27904.

Wellesen, K., Durst, F., Pinot, F., Benveniste, I., Nettesheim, K., Wisman, E., Steiner-Lange, S., Saedler, H. and Yephremov, A. (2001) Functional analysis of the *LACERATA* gene of Arabidopsis provides evidence for different robes of fatty acid omega-hydroxylation in development. *Proc. Natl Acad. Sci. USA*, **98**, 9694–9699.

Xiao, F.M., Goodwin, S.M., Xiao, Y.M., Sun, Z.Y., Baker, D., Tang, X.Y., Jenks, M.A. and Zhou, J.M. (2004) Arabidopsis CYP86A2 represses *Pseudomonas syringae* type III genes and is required for cuticle development. *EMBO J.* **23**, 2903–2913.

Xu, J.K., Liu, Y., Yang, Y.Y., Bates, S. and Zhang, J.T. (2004) Characterization of oligomeric human half-ABC transporter ATP-binding cassette G2. *J. Biol. Chem.* **279**, 19781–19789.

Yephremov, A., Wisman, E., Huijser, P., Huijser, C., Wellesen, K. and Saedler, H. (1999) Characterization of the *FIDDLEHEAD* gene of Arabidopsis reveals a link between adhesion response and cell differentiation in the epidermis. *Plant Cell*, **11**, 2187–2202.

Zheng, H., Rowland, O. and Kunst, L. (2005) Disruptions of the Arabidopsis enoyl-CoA reductase gene reveal an essential role for very-long-chain fatty acid synthesis in cell expansion during plant morphogenesis. *Plant Cell*, **17**, 1467–1481.

Zimmermann, P., Hirsch-Hoffmann, M., Hennig, L. and Gruissem, W. (2004) GENEVESTIGATOR. Arabidopsis microarray database and Analysis Toolbox. *Plant Physiol.* **136**, 2621–2632.

